18TH WORLD CONFERENCE ON EARTHQUAKE ENGINEERING
WCEE2024
MILAN

MILAN, ITALY
30TH JUNE - 5TH JULY 2024
www.wcee2024.it

SYSTEM AND COMPONENTS LEVEL SEISMIC PERFORMANCE ASSESSMENT OF SELF-CENTERING STEEL-CONCRETE HYBRID COUPLED WALLS

M. Farahi[1], F. Freddi[2] & M. Latour[3]

[1] Department of Civil, Environmental & Geomatic Engineering, Univ. College of London, UK, Mojtaba.farahi@ucl.ac.uk

[2] Department of Civil, Environmental & Geomatic Engineering, Univ. College of London, UK

[3] Department of Civil Engineering, University of Salerno, Italy

Abstract: *Several innovative structural solutions have been proposed in the last few decades to address the demand for seismic-resilient constructions. These solutions aim to minimize residual deformations and accelerate the repair process of structures after extreme seismic events. In this context, the present study investigates the seismic performance of an innovative seismic-resilient steel-concrete composite solution in which reinforced concrete shear walls coupled with self-centering steel beams, i.e., self-centering coupled wall systems (SC-CWs). The target coupling beams feature a friction-damped self-centering mechanism, which dissipates the seismic energy and contributes to the residual drift reduction, hence facilitating the repair of the structure after major earthquakes. 5- and 8-story SC-CWs are designed and considered for case study purposes. Non-linear finite element models are developed in OpenSees to perform non-linear static and dynamic analyses. Non-linear time-history analyses are performed in an Incremental Dynamic Analysis (IDA) fashion to evaluate the seismic response of each configuration, also accounting for the seismic input uncertainty, i.e., the record-to-record variability. Global and Local Engineering Demand Parameters (EDPs) are monitored to develop system- and component-level fragility curves. The results provide insights into the seismic response of SC-CWs, considering several damage states. The results are also compared with those obtained for similar CWs with replaceable links.*

1. Introduction

Coupled reinforced concrete (RC) walls are known as a common lateral load-resisting system for medium- to high-rise buildings in seismic-prone regions due to their superior strength and stiffness. Inelastic deformations (*i.e.,* damage) of coupling beams and the base of RC walls are the primary energy dissipation mechanism in coupled walls (Shahrooz et al. 1993, El-Tawil et al. 2010), often leading to large residual deformations after severe earthquakes (Wang 2008, Wallace et al. 2012, Westenenk et al. 2012). Excessive damage and residual deformations make structural repair difficult and time-consuming, if not impossible. This study aims to address this issue by proposing and investigating a structural solution to improve the energy dissipation capacity of coupled walls while, at the same time, limiting the earthquake-induced residual deformations, hence facilitating structural repairability.

The use of Self-Centering (SC) mechanisms has been proven as an effective strategy to reduce residual deformations and has been investigated in many structural configurations and different materials, including

steel moment-resisting frames (Ricles et al. 2002, Freddi et al. 2017, Dimopoulos et al. 2020, Elettore et al. 2021), braced frames (*e.g.,* O'Reilly and Goggins (2021), Lettieri et al. (2023)), RC structures (*e.g.,* Kurama et al. (2006), Zareian et al. (2020)), timber structures (*e.g.,* Pei et al. (2019), Blomgren et al. (2019)), and bridge piers (e.g.,Shen et al. (2023), Shen et al. (2022)). However, only a few studies focused on implementing such systems within RC-coupled walls, which represent more suitable solutions for taller buildings. Kurama et al. (2006) suggested the use of un-bonded Post-Tensioned (PT) tendons passing through the width of RC walls for connecting coupling beams. This connection allows the opening of a gap at beam-to-wall interfaces as the tension in the tendons exceeds their post-tensioning force under extreme lateral loadings, while the gap is closed after loading due to the restoring force provided by PT tendons. This solution was also experimentally investigated . Zareian et al. (2020) used unbonded PT bars and steel coupling beams to improve the seismic performance of coupled systems with friction dampers at beam-to-wall connections. However, the efficiency of this solution could be undermined by the elongation of coupling beams under large deformations, which could cause excessive local compressive stresses and damage at the connection with the RC wall (Weldon and Kurama 2010, Xie *et al*. 2023). In addition, the proposed SC coupling beams require on-site post-tensioning, which adds to the construction complexity and response uncertainties.

In order to reduce the residual deformation and improve the seismic resilience of steel-concrete composite coupled walls, steel coupling beams featuring a novel Friction Damped Self Centering (FDSC) link are used in this study. The proposed composite seismic-resisting system is referred to as Self-Centering Coupled Wall (SC-CW), and its seismic performance is numerically investigated in this study. Vertical PT bars providing the restoring force and friction devices (FDs) providing energy dissipation capacity are implemented in the intended FDSC links. PT bars are used in combination with disk springs to calibrate the deformability and resistance of the FDSC link and allow flexibility within the dimension of coupling beams. The FDSC link offers key advantages, including: 1) large and controlled energy dissipation capacity; 2) self-centering capability of the system; 3) easy reparability; 4) eliminates problems related to the coupling beams elongation; 5) facilitates the application of prefabricated SC components, which mitigates uncertainties raised by post-tensioning the connections on site.

In this paper, a 5- and a 8-story archetypes coupled systems are considered to investigate and compare the seismic performance of SC-CWs and their conventional CW counterparts with replaceable steel links. The seismic performance of the archetype SC-CWs is investigated through non-linear static and Incremental Dynamic Analyses (IDAs), and its advantages as an alternative seismic-resisting structural system are highlighted by comparing the results with equivalent structures with CWs and replaceable links. Furthermore, fragility curves are developed with respect to global and local Engineering Demand Parameters (EDPs) to examine the performance of the structures and evaluate the damages expected at components level.

2. Self-centering coupled walls

The application of steel beams for coupling RC shear walls has been proven to be an efficient strategy to improve the ductility of coupled walls (Ji et al. 2017), and current standards include design provisions for designing coupling steel beams, the required embedment in RC wall and the embedment details (AISC 2016). In this study, the configuration depicted in Figure 1 is used for steel coupling beams, which consist of two beam segments and an internal link. The side beam segments are designed to remain elastic, while the non-linear behavior expected under severe lateral loading is concentrated in the links. For the sake of comparison, the replaceable and FDSC links use the same design properties in this study.

As schematically shown in Figure 2 (a) and (b), the FDSC link is composed of two L-shaped and one T-shaped steel pieces, which are fixed to the adjacent beam segments to form the coupling beams. Symmetrical FDs are realized by adding friction pads between the T- and L-shaped pieces, pre-stressed with high-strength bolts. The length of the slotted holes in the web of the T-shaped pieces (Figure 2 (a)) is designed to accommodate the design target rotation/displacement (d_t). Vertical PT bars with disk springs shown in Figure 2 (c) are implemented to clamp the top and bottom anchorage plates and integrate the link under service load while providing the restoring force required to achieve the SC behavior of the link under extreme loading. Disk springs are arranged in parallel and series (Figure 2 (c)) to allow calibration of resistance and deformability of the FDSC links.

Figure 2 (d) schematically represents the flag-shaped shear force *vs*. displacement ($V_l - \Delta_l$) behavior of the FDSC link. As long as the shear force in the FDSC link (V_l) is less than the combination of the total post-

tensioning force in the PT bars (F_{PT}) and the frictional resistance (F_{FD}), the shear deformation of the FDSC link remains negligible in comparison with the shear deformation of the beam segments. That is, the shear-deformation behavior of the FDSC links is considered rigid-plastic (Figure 2 (d)). If V_l exceeds $F_{PT} + F_{FD}$ under extreme loading, a gap is opened between the anchorage plates and the T- and L-shaped pieces at opposite corners (Figure 2 (a)). The shear force at the onset of gap opening is referred to as the activation force ($F_{act} = F_{FD} + F_{PT}$). The stiffness of the FDSC links when the gap is open, K_{eq}, is estimated based on the stiffness of the PT bars and disk springs arranged in parallel and series. K_{eq} is reduced by arranging disk springs in series, which also decreases the elastic deformation demand on PT bars during the gap-opening phase.

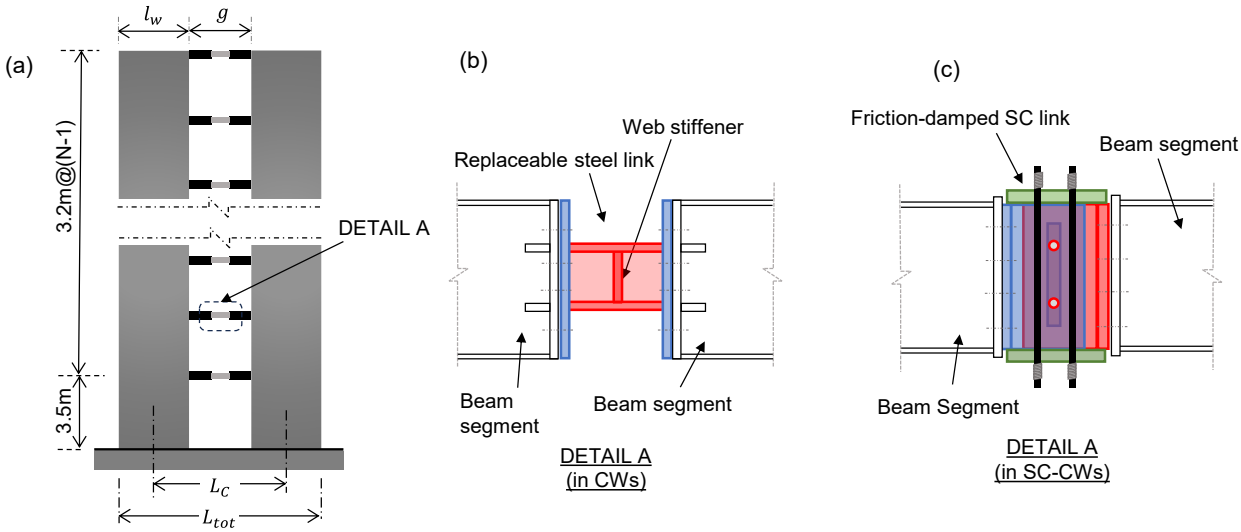

Figure 1. (a) The coupled wall configuration of interest with the main geometric parameters; (b) Coupling beams of CWs; (c) Coupling beams of SC-CWs.

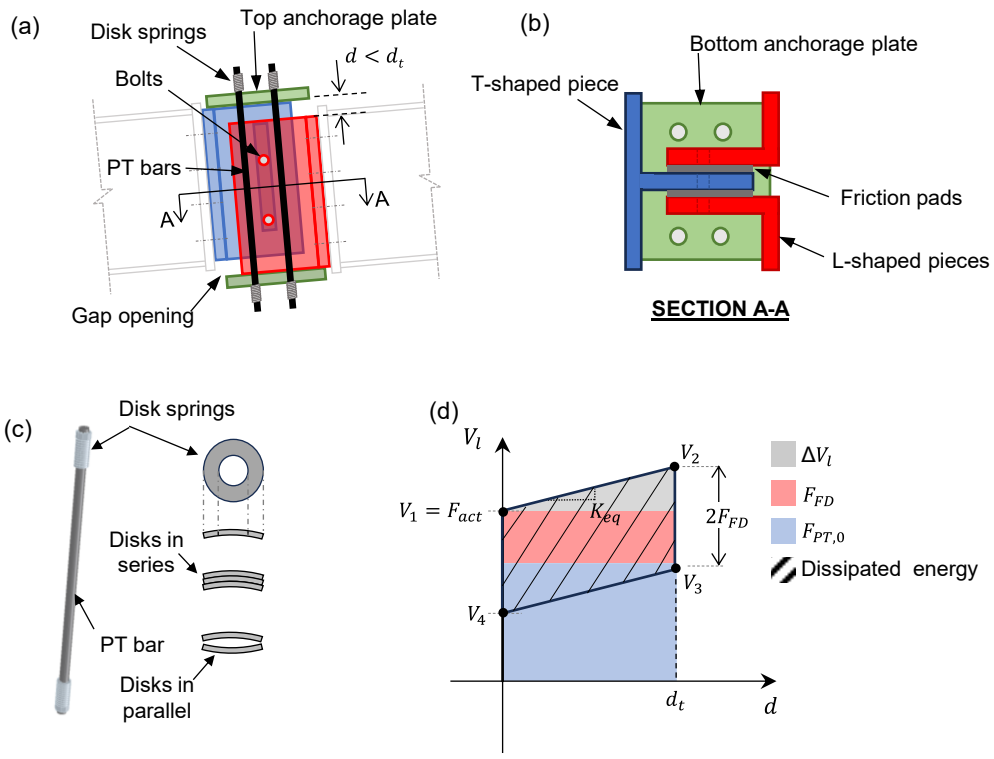

Figure 2. (a)Schematic representation of the FDSC link; (b) Section view of the FDSC link; (c) parallel and series arrangement of disk springs; (d) Flag-shaped shear force-deformation response of the FDSC link.

3. Design of archetype CWs/SC-CWs

Archetype CWs/SC-CWs designed and analyzed in this study are assumed to be the lateral load-resisting system of 5- and 8-story building with the plan view shown in Figure 3 (a) (Pieroni et al. 2022). The permanent (dead) and live gravity loads were considered equal to 4.5 and 2 kN/m^2, respectively.

A Performance-Based Design Method (PBDM) providing the framework for selecting performance objectives is used to design the archetypes (El-Tawil et al. 2010). The PBDM framework also allows controlling the coupling ratio (CR) for the archetypes to simultaneously achieve 'good' economy and structural performance. The CR in coupled wall systems is defined as the ratio of the bending moment resisted by the coupling action (tensile and compressive force in RC walls) to the total resisted bending moment. In prescriptive design procedures applied for common structural systems, the elastic properties are initially assumed according to current design standards. This procedure is followed by considering different geometries until the final design strength and stiffness meet the predicted demands. Hence, the CR results from the design procedure and is not chosen as a design parameter. On the contrary, any structural configuration can be proposed with a pre-defined CR within the performance-based approach. The proposed configuration is verified to ensure the resulting system meets the required performance objectives. If not, design iterations are conducted considering the same pre-defined CR until the required solution is achieved.

El-Tawil et al. (2010) proposed the following steps for the preliminary proportioning of a coupled wall system to minimize the required iterations. In the first step, the target CR is chosen, while the dimensions of RC walls are generally specified based on architectural specifications or available structural recommendations (for instance, Zona et al. (2016) recommended a height-to-width ratio of 10 for the RC walls in coupled systems). As the next step, the Overturning Moment (OTM) is initially estimated by the equivalent lateral force analysis according to current standards (ASCE 2017). Using the assumed CR value and the OTM calculated in the previous step, the coupling action or the summation of shear force in all coupling beams is estimated as $\sum_{i=1}^{N} V_{link,i} = CR \times OTM/L_C$, where L_C is the distance between the RC wall centroids (Figure 3), and N is the number of stories. For short to medium-rise building with low contribution of higher modes in their dynamic response, it can be assumed that the coupling action can be distributed uniformly along the building height (El-Tawil et al. 2010). As the third step, the force distribution along the RC walls shall be determined. To obtain the force distribution along the walls, El-Tawil et al. (2010) recommended releasing the coupling beams' end and applying the coupling beam end forces directly to the walls, as shown in Figure 3 (b). V_i and M_i at the interface of coupling beams and walls are equal to $V_{link,i}$ and $V_{link,i} \times g/2$, where g is the length of coupling beams. In the final step, the RC walls, beam segments, and FDSC links can be designed for the internal forces evaluated in the previous steps. It is worth mentioning that the maximum axial force in the compression wall should be less than 35% of the pier's axial capacity to account for the detrimental effects of beam overstrength and to ensure the axial stability of the RC walls (El-Tawil et al. 2010). The efficiency of the design to fulfill the performance objective is finally checked through performing non-linear static analysis.

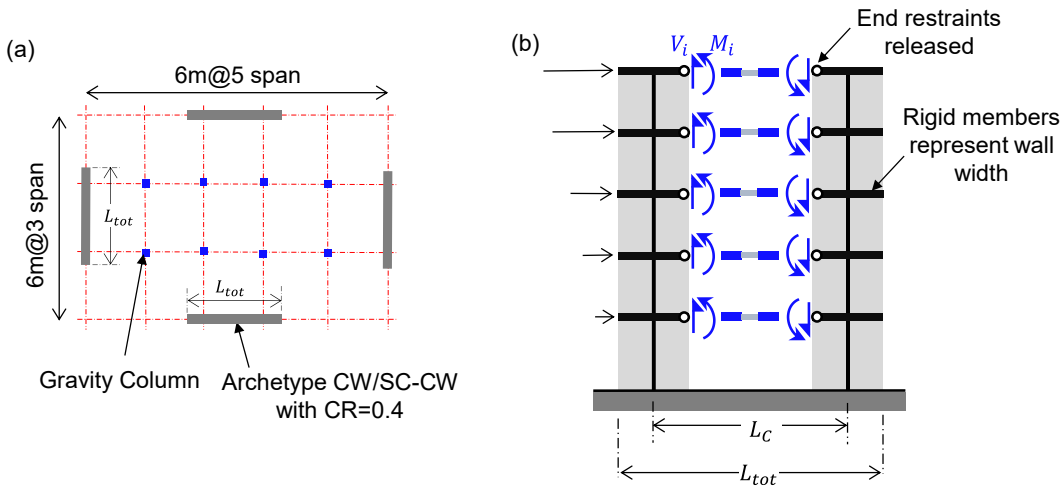

Figure 3. (a) Plan of the case study building; (b)Idealized elastic model used for preliminary proportioning of coupled walls (El-Tawil et al. 2010).

Two 5- and 8-story archetype SC-CWs and their equivalent CWs counterparts with replaceable steel links are designed with a pre-defined coupling ratio of 40% and assuming a peak ground acceleration of 0.35g according to (ASCE 2017). Table 1 reports the design results for the archetypes in this study, and the properties of the FDSC links have been summarized in Table 2.

Table 1. Design outcomes for the archetypes considered in this study.

	CW-5Story	SC-CW-5Story	CW-8Story	SC-CW-8Story
Wall width [mm]	2500		4000	
Wall boundary width [mm]	600		1000	
Wall thickness [mm]	350		400	
Vertical reinforcement density in the web [-]	0.005		0.004	
Vertical reinforcement density in the boundary elements [-]	0.033		0.022	
Links section	IPE 240	FDSC1	IPE 240	FDSC1

Table 2. The properties of the FDSC links.

	PT bars	Post-tension force in each bar [kN]	Friction resistance force, F_{FD} [kN]	Activation force, F_{act} [kN]	Equivalent post-activation stiffness, K_{eq} [kN/mm]
SCHCW-W3.2-U	M16, Grade 10.9	52	110	317	6

4. Finite Element (FE) modeling methodology

2D non-linear models of the archetypes were developed in OpenSees (McKenna et al. 2000). Figure 4 provides a schematic representation of the FE modeling approach implemented in this study. The 2D Shear-Flexure Interaction Multiple-Vertical-Line-Element-Model (SFI-MVLEM) (Kolozvari et al. 2018) is implemented to model RC shear walls. This model is based on a fiber-based formulation and incorporates a biaxial constitutive panel behavior. This model also accounts for the axial force-shear interaction, which cannot be ignored in the simulation of RC walls subjected to lateral loading. SFI-MVLEM has been verified for RC walls in coupled systems, and the modeling parameters suggested by Kolozvari et al. (2018) were used in this study. The RC walls of the archetype SC-CWs are discretized to 19 fibers (panels) across their width to represent the walls' cross-section and reinforcements arrangement in the boundary and web areas. 'ConcreteCM' and 'Steel02' material models in OpenSees were implemented within the SFI-MVLEM as the constitutive relationships for concrete and reinforcement, respectively. OpenSees 'MinMax' wrapper is also used in conjunction with 'Steel02' material to simulate the tensile fracture of reinforcing bars by reducing their material strength to zero once the reinforcement tensile strain exceeds an ultimate value of 0.05 (Gogus and Wallace 2015).

The 'Elastic BeamColumn Elements' in OpenSees are used to model the beam segments of the coupling beams. In addition, 'zero-length' shear springs with an elastic stiffness equal to the beam segment cross-section are defined at their connection to the wall. The shear springs account for the elastic shear deformation of the beam segments. The FDSC links are modeled using 'Two-Nodes Link Elements'. The mechanical behavior of 'Two-Nodes Link Elements' is determined by the Uni-directional materials assigned to three springs representing the links' degrees of freedom. The axial and flexural deformation of FDSC links are assumed to be negligible (FDSC links are rigid with respect to axial and flexural degrees of freedom), while the 'Self-Centering Uniaxial material' from OpenSees material library is utilized to represent the flag-shaped shear-deformation behavior depicted in Figure 2 (d).

In addition, a dummy column connected to each archetype model with rigid truss elements at every story is also modeled to account for the second-order effects imposed on the archetypes from the gravity system of the case-study building. This dummy column carries a portion of the floor weight at each level, which is not transferred directly to the archetype.

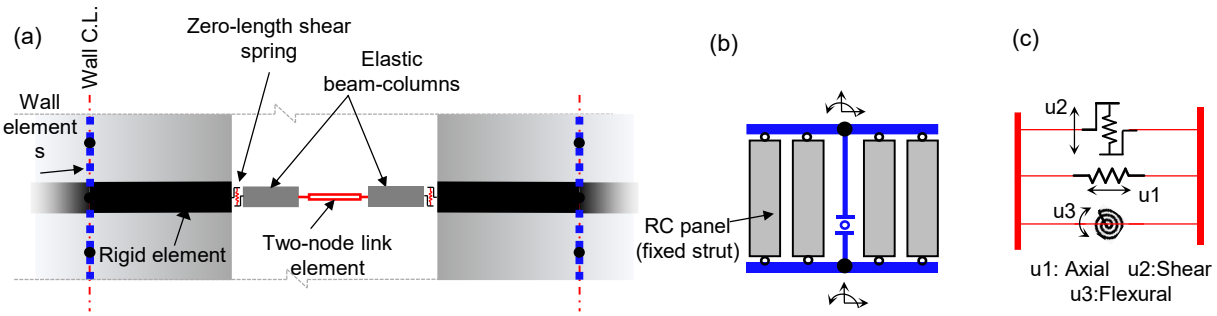

Figure 4. (a) Schematic representation of finite element modeling; (b) Wall elements, SFI-MVLEM (Kolozvari et al. 2018); (c) Two-node link element.

5. Non-linear Analyses

Non-linear static and dynamic (time-history) analyses are conducted on the numerical models prepared for the archetype CWs/SC-CWs to investigate their seismic performance and to assess the sufficiency of the performance-based design approach used to design the archetypes.

Figure 5 shows the outcomes of the static non-linear analyses for the archetypes in the form of pushover curves. Some critical points are highlighted on the curves, including: 1) the roof drifts at which the first and the last link yield/activate and reach the chosen chord rotation. The chord rotation limit is considered equal to 0.08 rad in this study based on the rotation limit for short steel links suggested by AISC (2016); 2) the onset of concrete crushing, when the confined concrete strain in boundary regions exceeds 0.005 and/or the concrete reaches its maximum compression strength; 3) the steel reinforcement failure when the tensile strain in steel rebars exceeds 0.05 according to Gogus and Wallace (2015). This situation is associated with the wall collapse limit state.

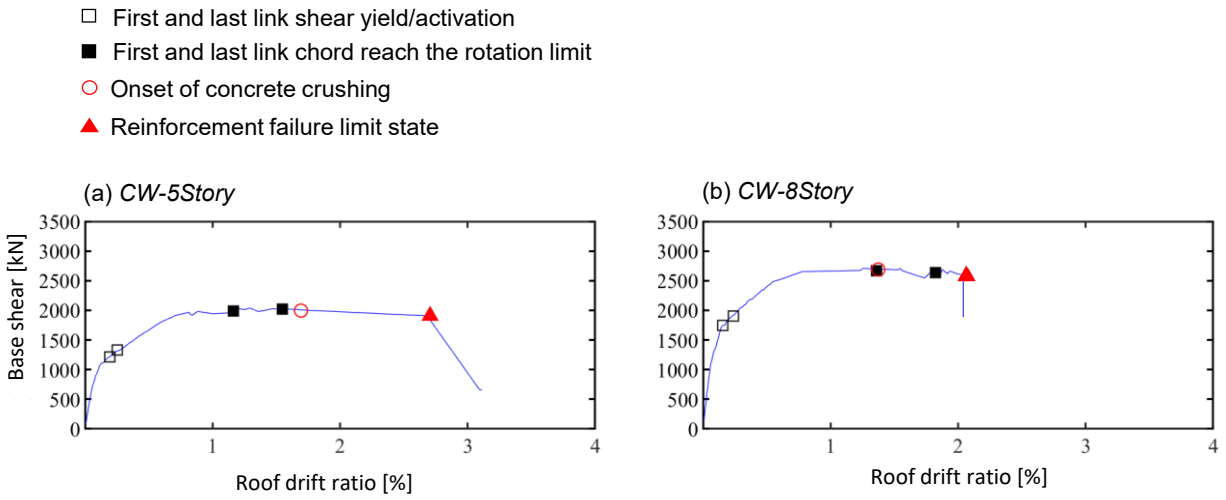

Figure 5. Pushover curves for (a) 5-story and (b) 8-story archetypes.

The yield base shear for all archetype models obtained from the models was consistent with their design base shear. The yield mechanism started with the shear yield of replaceable links or the activation of the FDSC links according to the design procedure, and the links reached their rotation limit (assumed failure limit) before the failure of the RC walls. Furthermore, the activation and failure of the links at different levels happened quite at the same time. These two observations from the results of the non-linear static analyses lead to the conclusion that the links contribute effectively to the dissipation of input energy, and the damage is concentrated in these members before the critical damages emerge in the RC walls.

The seismic performance of the archetype models is also evaluated by performing Incremental Dynamic Analyses (IDAs) in which the models are subjected to various ground motion records with increasing intensities

(Vamvatsikos and Cornell 2002). The far-field ground motion records set suggested by FEMA P695 (2009), and including 22 pairs of records, are used to perform the IDAs. The Intensity Measure (IM) is selected as the spectral acceleration at the fundamental period, $Sa(T_1)$ in this research. The natural vibration periods for the two 5-story and 8-story archetypes were respectively equal to $T_{1,5\,Story} = 0.55$ and $T_{1,8\,Story} = 0.78$ sec.

Figure 6 shows the distribution of peak interstory drifts and residual interstory drifts along the height of the archetype models. The profiles in these figures represent the median of the results obtained for all ground motion records at the Design Basis Earthquake (DBE) and Maximum Credible Earthquake (MCE) intensity levels (dashed and solid lines respectively). DBE and MCE spectral values were calculated according to ASCE (2017) in this study. The comparison between the median peak interstory drifts obtained for the 5- and 8-story CWs and SC-CWs shows that SC-CWs are prone to slightly larger peak drifts compared with their counterpart CWs with conventional steel links. This can be justified by referring to the smaller energy dissipation capacity of FDSC links with flag-shaped hysteresis behavior compared with the replaceable links with full hysteresis behavior (Lettieri et al. 2023). This shortcoming can be overcome by increasing the post-activation stiffness of FDSC links at the design stage. On the other hand, Figure 6 (b) and (d) shows the effective performance of FDSC links in restoring the earthquake-induced residual interstory drifts. The significant reduction in the residual deformations in SC-CWs leads to better repairability and superior seismic-resilience compared with their conventional counterparts.

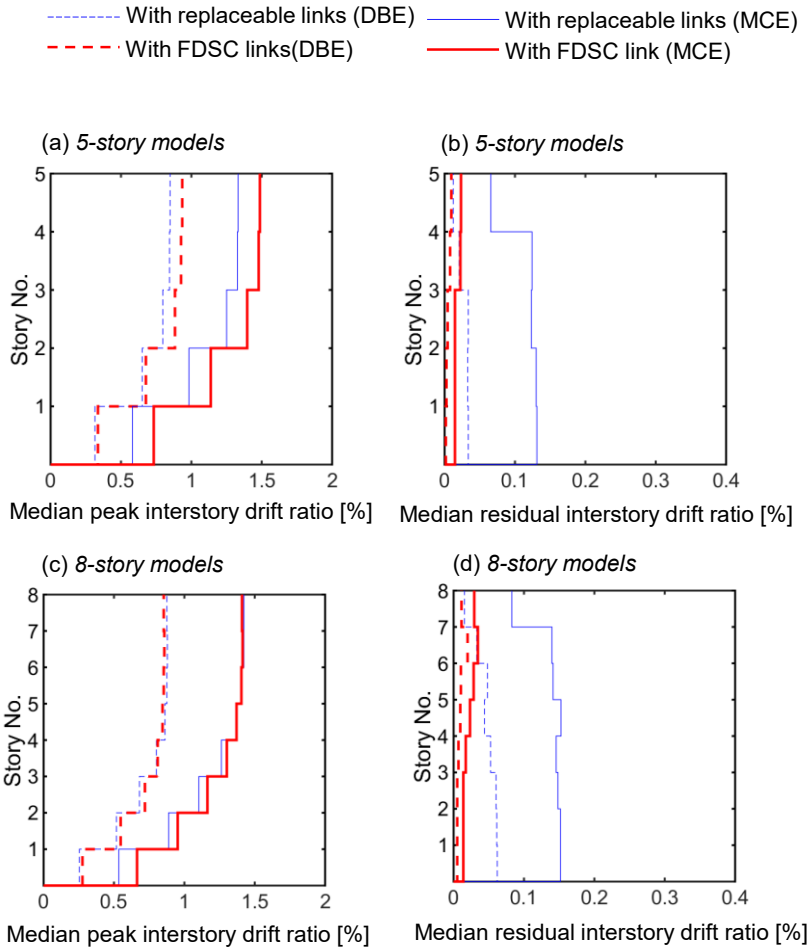

Figure 6. (a) Median peak interstory drift along the height of the 5-story archetypes; (b) Median residual interstory drift along the height of 5-story archetypes; (c) Median peak interstory drift along the height of the 8-story archetypes; (d) Median residual interstory drift along the height of 8-story archetypes.

Figure 7 shows the fragility curves based on local Engineering Demand Parameters (EDPs) for the ultimate links chord rotation ($\theta_{chord,L,ls} = 0.08$ rads) and the ultimate rebars tensile strain ($\varepsilon^{w}_{s,ls} = 0.05$) limit states.

These curves are developed by fitting log-normal curves to the fragility data points through least-square minimization.

The comparison of fragility curves in Figure 7 for the SC-CWs and CWs confirms that the application of the intended FDSC links did not significantly increase the probability of the reinforcement failure as a dominant failure mode of RC walls (about 10% and 15% at MCE intensity for 5- and 8-story archetypes respectively). However, this shortcoming can be addressed by selecting higher post-activation stiffness values for the FDSC links or adopting larger friction forces (higher energy dissipation capacity) at the design stage. It is also worth noting that the global failure is governed by the exceedance of the links chord rotation limit, 0.08 rad according to Figure 7. Although this limit state is set based on the standard limitation for steel short links evidenced by experimental findings, FDSC links can be designed to allow larger rotations (gap opening). That is, by choosing a realistic and larger rotation capacity for FDSC links, the probability of exceedance of the links rotation limit will be reduced (red dashed curves approach the blue dashed curves).

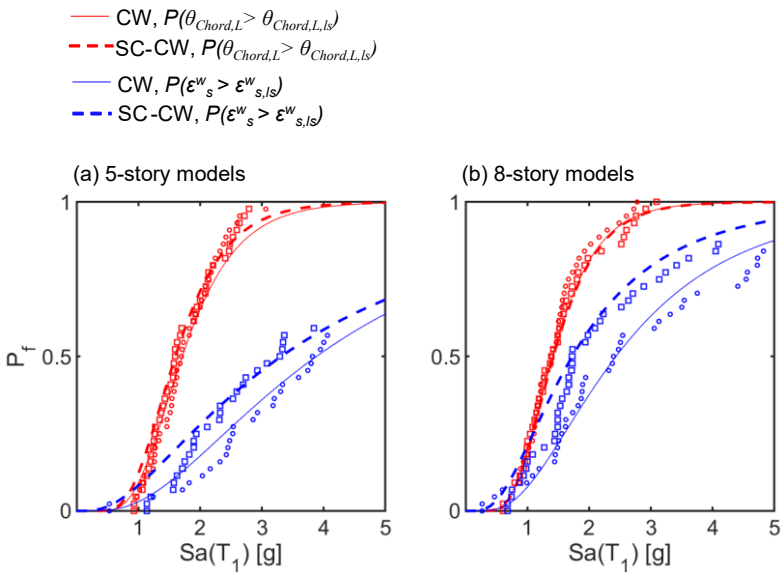

Figure 7. Probability of exceedance of links chord rotation of $\theta_{chord,L,c}$ (red curves); rebars strain of $\varepsilon_{s,ls}^{w} = 0.05$ (blue curves) for (a) 5-story archetypes (b) 8-story archetypes.

6. Conclusions

The results of a numerical investigation on the seismic performance of self-centering coupled walls (SC-CWs) were summarized in this paper, and the capability of SC-HWs in minimizing earthquake-induced residual deformations was elaborated. The efficiency of SC-CWs as novel lateral load-resisting systems was proved compared with the performance of coupled walls (CW) with steel coupling beams as their counterparts. Comparing the results obtained for the 5- and 8-story archetype SC-CWs and CWs highlighted that a significant reduction in residual deformations could be achieved by using the Friction-Based Self-Centering (FBSC) links without considerable exacerbation of the damage to the RC walls. It is worth mentioning that the properties of FDSC links can be calibrated in future studies to reduce the damage to RC walls and improve the seismic resilience of SC-CWs. It is worth highlighting that the configuration of the proposed FDSC links can allow larger relative vertical deformations (chord rotations). Further experimental studies have been planned to prove a deformability limit larger than 0.08 rad for the proposed FDSC links.

7. Acknowledgment

This research was supported by the European Union's Horizon 2020 research and innovation program under grant agreement No. 101027745 (Marie Sklodowska-Curie Research Grant Scheme H2020-MSCA-IF-2020: Self-Centering Earthquake-Resilient Hybrid Steel-Concrete Shear Walls with Rocking Beams - SC-HYBWalls). The Authors also acknowledge the support from the Royal Society - International Exchange programme under

the grant agreement IES\R3\213175. Any opinions, findings, conclusions and/or recommendations expressed in this paper are those of the authors and do not necessarily reflect the views of the Funders.

8. References

AISC (2016). Specification for structural steel buildings, AISC, Chicago.

ASCE (2017). Seismic evaluation and retrofit of existing buildings, Reston, VA.

Blomgren, H.-E., Pei, S., Jin, Z., Powers, J., Dolan, J. D., Lindt, J. W. v. d., Barbosa, A. R., and Huang, D. (2019). Full-scale shake table testing of cross-laminated timber rocking shear walls with replaceable components. *Journal of Structural Engineering*, 145(10), 04019115.

Dimopoulos, C. A., Freddi, F., Karavasilis, T. L., and Vasdravellis, G. (2020). Progressive collapse resistance of steel self-centering MRFs including the effects of the composite floor. *Engineering Structures*, 208, 109923.

El-Tawil, S., Harries, K. A., Fortney, P. J., Shahrooz, B. M., and Kurama, Y. (2010). Seismic design of hybrid coupled wall systems: *state of the art. Journal of Structural Engineering*, 136(7), 755-769.

Elettore, E., Freddi, F., Latour, M., and Rizzano, G. (2021). Design and analysis of a seismic resilient steel moment resisting frame equipped with damage-free self-centering column bases. *Journal of Constructional Steel Research*, 179, 106543.

FEMA (2009). Quantification of building seismic performance factors. FEMA P695Washington, DC: FEMA.

Freddi, F., Dimopoulos, C. A., and Karavasilis, T. L. (2017). Rocking damage-free steel column base with friction devices: design procedure and numerical evaluation. *Earthquake Engineering & Structural Dynamics*, 46(14), 2281-2300.

Gogus, A., and Wallace, J. W. (2015). Seismic safety evaluation of reinforced concrete walls through FEMA P695 methodology. *Journal of Structural Engineering*, 141(10), 04015002.

Ji, X., Liu, D., Sun, Y., and Molina Hutt, C. (2017). Seismic performance assessment of a hybrid coupled wall system with replaceable steel coupling beams versus traditional RC coupling beams. *Earthquake Engineering & Structural Dynamics*, 46(4), 517-535.

Kolozvari, K., Orakcal, K., and Wallace, J. W. (2018). New OpenSees models for simulating nonlinear flexural and coupled shear-flexural behavior of RC walls and columns. *Computers & Structures*, 196, 246-262.

Kolozvari, K., Terzic, V., Miller, R., and Saldana, D. (2018). Assessment of dynamic behavior and seismic performance of a high-rise rc coupled wall building. *Engineering Structures*, 176, 606-620.

Kurama, Y. C., Weldon Brad, D., and Shen, Q. (2006). Experimental evaluation of posttensioned hybrid coupled wall subassemblages. *Journal of Structural Engineering*, 132(7), 1017-1029.

Lettieri, A., de la Peña, A., Freddi, F., and Latour, M. (2023). Damage-free self-centring links for eccentrically braced frames: development and numerical study. *Journal of Constructional Steel Research*, 201, 107727.

McKenna, F., Fenves, G., Scott, M., and Jeremic, B. (2000). Open system for earthquake engineering simulation (OpenSees). Pacific Earthquake Engineering Research Center, UC Berkeley (CA).

O'Reilly, G. J., and Goggins, J. (2021). Experimental testing of a self-centring concentrically braced steel frame. *Engineering Structures*, 238, 111521.

Pei, S., van de Lindt John, W., Barbosa Andre, R., Berman Jeffrey, W., McDonnell, E., Daniel Dolan, J., Blomgren, H.-E., Zimmerman Reid, B., Huang, D., and Wichman, S. (2019). Experimental seismic response of a resilient 2-story mass-timber building with post-tensioned rocking walls. *Journal of Structural Engineering*, 145(11), 04019120.

Pieroni, L., Freddi, F., and Latour, M. (2022). Effective placement of self-centering damage-free connections for seismic-resilient steel moment resisting frames. *Earthquake Engineering & Structural Dynamics*, 51(5), 1292-1316.

Ricles, J. M., Sause, R., Peng, S. W., and Lu, L. W. (2002). Experimental evaluation of earthquake resistant posttensioned steel connections. *Journal of Structural Engineering*, 128(7), 850-859.

Shahrooz, B. M., Remmetter, M. E., and Qin, F. (1993). Seismic design and performance of composite coupled walls. *Journal of Structural Engineering (ASCE)*, 119(11), 3291-3309.

Shen, Y., Freddi, F., Li, Y., and Li, J. (2023). Enhanced strategies for seismic resilient posttensioned reinforced concrete bridge piers: experimental tests and numerical simulations. *Journal of Structural Engineering*, 149(3), 04022259.

Shen, Y., Freddi, F., Li, Y., and Li, J. (2022). Parametric experimental investigation of unbonded post-tensioned reinforced concrete bridge piers under cyclic loading. *Earthquake Engineering & Structural Dynamics*, 51(15), 3479-3504.

Vamvatsikos, D., and Cornell, C. A. (2002). Incremental dynamic analysis. *Earthquake Engineering & Structural Dynamics*, 31(3), 491-514.

Wallace, J. W., Massone, L. M., Bonelli, P., Dragovich, J., Lagos, R., Lüders, C., and Moehle, J. (2012). Damage and implications for seismic design of RC structural wall buildings. *Earthquake Spectra,* 28(SUPPL.1), S281-S299.

Wang, Y. (2008). Lessons learned from the 5.12 Wenchuan Earthquake: evaluation of earthquake performance objectives and the importance of seismic conceptual design principles. Earthquake *Engineering and Engineering Vibration*, 7(3), 255-262.

Weldon, B. D., and Kurama, Y. C. (2010). Experimental evaluation of posttensioned precast concrete coupling beams. *Journal of Structural Engineering*, 136(9), 1066-1077.

Westenenk, B., de la Llera, J. C., Besa, J. J., Jünemann, R., Moehle, J., Lüders, C., Inaudi, J. A., Elwood, K. J., and Hwang, S.-J. (2012). Response of reinforced concrete buildings in concepción during the maule earthquake. *Earthquake Spectra*, 28(1_suppl1), 257-280.

Xie, C., Wang, X., and Vasdravellis, G. (2023). Mechanical behaviour and experimental evaluation of self-centring steel plate shear walls considering frame-expansion effects. *Journal of Building Engineering*, 72, 106636.

Zareian, M. S., Esfahani, M. R., and Hosseini, A. (2020). Experimental evaluation of self-centering hybrid coupled wall subassemblies with friction dampers. *Engineering Structures*, 214, 110644.

Zona, A., Degée, H., Leoni, G., and Dall'Asta, A. (2016). Ductile design of innovative steel and concrete hybrid coupled walls. *Journal of Constructional Steel Research*, 117, 204-213.